

# Reliability-Based Design Guidelines for Fatigue of Ship Structures

Bilal M. Ayyub<sup>1</sup>, Ibrahim A. Assakkaf<sup>2</sup>, David P. Kihl<sup>3</sup>, and Michael W. Sieve<sup>4</sup>

## ABSTRACT

Marine and offshore structures are subjected to fatigue loadings primarily due to the action of seawater waves and the sea environment in general. The load cycles in such an environment can be in the order of a million cycles per year. Fatigue failures in these structures can take place at sites of high stress concentration that can be classified into two major categories: baseplate and weldments. The former includes locations of high stress concentration such as openings, sharp re-entry corners, and plate edges. In general, the mechanisms behind these failures are described by the general approaches to fatigue life prediction as discussed in this paper. There are two major approaches for predicting fatigue life: (1) the *S-N* curve approach and (2) the fracture mechanics (FM) approach. The *S-N* curve approach is based on experimental measurement of fatigue life in terms of cycles to failure for different loading levels and specimen geometries, while the fracture mechanics (FM) approach is based on the existence of an initial crack and subsequent crack propagation under cyclic load.

The objective of this paper is to develop reliability-based methods for determining the fatigue life of structural details associated with conventional displacement type surface monohull ships based on the *S-N* approach and on the assumption that fatigue damage accumulation is a linear phenomenon (i.e., that follows Miner's rule). The methods are also based on structural reliability theory and can be applied either in direct reliability-based design or in a load and resistance factor design (LRFD) format. The resulting design methods are referred to as the

---

<sup>1</sup>Contact author, Professor & Director, Center for Technology & Systems Management, Department of Civil & Environmental Engineering, University of Maryland, College Park, MD 20742, 301-405-1956 (Tel), ayyub@umail.umd.edu

<sup>2</sup>Center for Technology and Systems Management, Department of Civil and Environmental Engineering, University of Maryland, College Park, MD 20742.

<sup>3</sup>Surface Ship Structures Department, Naval Surface Warfare Center - Carderock Division, Code 653, West Bethesda, MD 20817-5700.

<sup>4</sup>Structures, Naval Sea System Command, U. S. Navy, Washington Navy Yard, Building 197, 1333 Isaac Hull Avenue, S. E., Washington, DC 20376..

reliability-based design approach for fatigue of marine structures. These design methods were developed according to the following requirements: (1) spectral analysis of wave induced loads, (2) use of conventional fatigue design codes, (3) nominal strength and load values, and (4) achieving target reliability levels. The first-order reliability method (FORM) was used to perform reliability assessments and to develop the partial safety factors (PSF's) for fatigue limit state equations.

## **1. INTRODUCTION**

In recent years, a great deal of attention has focused on avoiding fatigue failure of ship structural details. The financial consequences and risks associated with this type of failure require structural engineers to consider fatigue strength in their designs, especially for those structural components that are exposed to cyclic loading. The term “fatigue” is commonly used in engineering to describe damage due to repeated-load application and its effect on the strength and structural integrity of a structural member. The exact mechanism of a fatigue failure is complex and is not completely understood. Failure by fatigue is a progressive irreversible cracking process, which unless detected and remedied, can lead to a catastrophic rupture (see Figures 1 and 2). When a repeated load is large enough or applied enough times to cause a fatigue crack, the crack will start at the point of maximum stress. This maximum stress is usually due a stress concentration (stress raiser). After a fatigue crack is initiated at some microscopic or macroscopic level of stress concentration, the crack itself can act as an additional stress raiser causing crack propagation. The crack grows with each repetition of the load until the effective cross section is reduced to such an extent that the remaining portion will fail with the next application of the load. For a fatigue crack to grow to such an extent to cause rupture, it may take thousands or even millions of stress applications, depending on the magnitude of the load, type of the material used, and on other related factors. A detailed bibliography for fatigue of welds was developed by the University of Tennessee (1985). However, this bibliography does not cover work beyond 1985.

Fatigue must be considered in the design of all-structural and machine components that are subjected to repeated or fluctuating loads. During the useful life of a structural member, the expected number of loading cycles varies tremendously. For example, a beam supporting a

crane may be loaded 2,000,000 times in 25 years to failure, while an automobile crankshaft might be loaded 5,000,000,000 times for rupture to occur, if the automobile is driven 200,000 miles (Beer and Johnston, 1981). The number of loading cycles required to cause failure of a structural component may be determined experimentally for any given applied change in stress level. One common test used to evaluate the fatigue properties of a material is a rotating-beam test (Byars and Snyder 1975). In this test, the number of completely reversed cycles of bending stress required to cause failure is measured at different stress levels. In one complete cycle, the stress changes from maximum tensile stress, to zero, to maximum compressive stress of the same magnitude as the maximum tensile stress, through zero again, and then back to the original maximum tensile stress. If a series of tests are conducted in this case, using different maximum stress ranges, the resulting data can be plotted as an  $S-N$  curve. For each test, the maximum stress range  $S$  is plotted against the number of cycles to failure  $N$ . These test data are usually plotted on log-log or semi-log paper, and the resulting plot is referred to as an  $S-N$  curve. Figure 3 shows typical curves for various materials. It is to be noted from these curves, that as the magnitude of the maximum stress range decreases, the number of cycles required to cause rupture increases. Also, these curves tend to follow approximately horizontal lines at low stress levels, defining a lower limit. When the stress level for a specimen reaches this limit, the specimen does not fail and it is said to have reached the endurance limit (fatigue limit). The endurance limit is then defined as the stress for which failure does not take place (Beer and Johnston, 1981) even for an indefinitely large number of loading cycles. The endurance limit for most engineering materials is much less than the yield strength. For a low carbon structural steel, the endurance limit is about half of the ultimate strength of the steel.

Fatigue properties for some materials are determined at high temperatures and also in various corrosive environments. Temperature and environment can play a drastic role in influencing the fatigue properties. For example, in applications in or near seawater, or in other applications where high level of corrosion is expected, a reduction up to 50% in the endurance limit may be anticipated. Also, since fatigue failure may be initiated at any crack or imperfection, the service condition of a specimen has a vital effect on the value of the endurance limit obtained in the test.

The inherent nature of fatigue tests gives rise to a great deal of scatter in the data. For example, if several specimens that have been carefully machined and polished, are tested at the

same stress level, it certainly not unusual to have a variation of 10 to 20 percent in their fatigue life measured in terms of the number of loading cycles at which the specimen ruptures (Byars and Snyder, 1975). It therefore requires many tests to adequately quantify an  $S-N$  curve for a given material.

Fatigue cracking of structural details in ship and offshore steel structures due to cyclic loading has gained considerable attention in recent years. Numerous research works have been conducted in this field on both theoretical and practical aspects. Consequently, a great deal of papers have been published resulting in various topics relating to fatigue assessment and prediction. In these papers, the macroscopic behavior of materials, as well as models for their description, are investigated. Due to the extreme complexity in modeling the process of material cracking at the microscopic level, solutions from the microscopic aspect are rarely available or not practically feasible. This is mainly due to the complexity of the damaging process under cyclic loading and the natural variation in material properties. Ship and offshore structures are subjected to fatigue primarily due to the action of seawater waves (Byers et al. 1997) and the sea environment in general. The load cycles in such an environment can be on the order of a million cycles per year.

Fatigue failures in ship and offshore structures can take place at sites of high stress concentration that can be classified into two major categories: (1) baseplate and (2) weldments. The former includes locations of high stress concentration such as openings, sharp re-entry corners, and plate edges. In general, the mechanisms behind these failures are described by the general approaches to fatigue life prediction. There are two major approaches for evaluating fatigue life prediction: (1) the  $S-N$  curve approach and (2) the fracture mechanics (FM) approach. The  $S-N$  curve approach is based on experimental measurement of fatigue life in terms of cycles to failure for different structural details and loading levels as discussed previously. On the other hand, the fracture mechanics (FM) approach is based on the existence of an initial crack and subsequent growth under cyclic loading. Both of these approaches are discussed in greater detail.

## **2. LIMIT STATES AND DESIGN STRENGTH**

There are two major technical approaches for fatigue analysis and design of welded joints: (1) the fracture mechanics approach and (2) the characteristic  $S-N$  curve approach. Both

of these approaches are discussed in the subsequent sections with the emphasis on the latter approach.

## 2.1 The Fracture Mechanics Approach

The fracture mechanics approach is based on crack growth data of an initial flaw of known (or assumed) size and geometry. For welded joints, it is assumed that an appropriate initial defect exists, which is just under the threshold of detection, fatigue life can then be predicted using the fracture mechanics method to determine the number of cycles required to grow the crack to a certain unstable growth. The fracture mechanics approach is more detailed and it involves examining crack growth and determining the number of load cycles that are needed for small initial defects to grow into cracks large enough to cause fracture. The growth rate is proportional to the stress range. It is expressed in terms of a stress intensity factor  $K$ , which accounts for the magnitude of the stress, current crack size, and weld and joint details. The basic equation that governs crack growth is given by

$$\frac{da}{dN} = C\Delta K^m \quad (1)$$

where  $a$  = crack size,  $N$  = number of fatigue cycles,  $\Delta K$  = range of stress intensity factor, and  $C$  and  $m$  are empirically derived crack propagation parameters. The range of the stress intensity factor is given by Broek (1986) as

$$\Delta K = SY(a)\sqrt{\pi a} \quad (2)$$

in which  $Y(a)$  is a function of crack geometry. When the crack size  $a$  reaches some critical crack size  $a_{cr}$ , failure is assumed to have occurred. Although most laboratory testing is performed with constant-amplitude stress ranges, Eq. 1 is typically applied to variable stress range models that ignore sequence effects (Byers et al. 1997). Rearranging the variables in Eq. 1, the number of cycles can be computed using the following equation:

$$N = \frac{1}{CS^m} \int_{a_0}^a \frac{da}{Y^m(a)(\sqrt{\pi a})^M} \quad (3)$$

Eqs. 1 and 3 involve a variety of sources of uncertainty (Harris 1995). The crack propagation parameter  $C$  in both equations is treated as a random variable (Madsen 1983). However, in more

sophisticated models, Eq. 1 is treated as a stochastic differential equation and  $C$  is allowed to vary during the crack growth process (Ortiz 1985 and Byers et al. 1997). Lin and Yang (1983) treated the crack growth as Markov process, while Ditlevsen (1986) treated it as a first-passage problem.

## 2.2 The Characteristic $S$ - $N$ Approach

The characteristic  $S$ - $N$  curve approach is based on fatigue test data ( $S$ - $N$  curves) as described in the introduction and on the assumption that fatigue damage accumulation is a linear phenomenon that is independent of previously applied cycles (i.e., that follows Miner's rule). According to Miner's rule, the total fatigue life under a variety of stress ranges is the weighted sum of the individual lives at constant stress  $S$  as given by the  $S$ - $N$  curves, with each being weighted according to fractional exposure to that level of stress range (Hughes 1988). Upon crack initiation, cracks propagate based on the fracture mechanics concept as shown in Figure 4.

The fatigue behavior of different types of structural details is generally evaluated in constant-cycle fatigue tests and the results are presented in terms of the nominal applied stresses and the number of cycles of loading that produce failure. The resulting  $S$ - $N$  curves are usually presented as straight lines on a log-log paper as shown in Figure 5. The basic equation that represents the  $S$ - $N$  curve is given by

$$N = \frac{A}{S^m} \quad (4)$$

where  $N$  = number of cycles to fatigue initiation (failure),  $A$  and  $m$  are empirical constants. Eq. 4 can also be expressed in a linear form as

$$\log N = \log A - m \log S \quad (5)$$

where  $\log$  is to the base 10. The fatigue strength can be computed over a range of lives covered by the straight line if the slope of the line and one point on the line are known. However, only one type of stress cycle and one detail are represented on an individual  $S$ - $N$  curve (Munse et al. 1983). In general, a least-squares analysis of  $\log N$  given  $S$  fatigue data is used to produce the  $S$ - $N$  curve and associated experimental constants,  $\log(A)$  and  $m$ .

The choice of appropriate stress history is an important factor in reliability-based design and analysis for fatigue. The question is not really how to determine the stress history; rather,

what constitutes an appropriate stress history. According to Moan and Berge (1997), and based on the terminology adapted by the International Institute of Welding (IIW) in 1996, the following four different approaches are classified for stress determination for fatigue design and analysis: (1) the nominal stress approach, (2) the hot spot stress approach, (3) the notch stress approach, and (4) the notch strain approach. Figure 6 shows a schematic of these approaches. Except for the nominal stress approach, the rest are commonly called local stress approaches. Probably the most common approaches for determining fatigue stresses in marine industry are the nominal stress and the hot spot approaches. These methods are discussed in the next section. For more detailed description of the notch stress and notch strain approaches, Section 2 (Fatigue and Fracture) of Moan and Berge (1997) provides such description.

### **2.3 Nominal Stress Versus Hot Spot Stress**

The nominal stress approach is the simplest one among the four approaches. In this approach, the stress is represented by an average loading of the whole structural detail under study. The nominal stress is the “far-field” stress due to forces, moments, or combinations of the two acting at the location of possible cracking site in the detail. In this approach, neither the weld toe geometry, nor the properties of the material constitutive relations are taken into consideration (Moan and Berge 1997). The  $S-N$  curve resulting from this analysis is unique to the structural detail for which it is established. It is possible to use one such curve to represent others similar details if there is insignificant variation in their geometry. Most current design codes divide various structural details into different classes and provide an  $S-N$  curve for each class. For example, the British Standards (BS 1980) and Norwegian Standards (1984) have eight classifications as shown in Table 1. However, for a more rigorous analysis, each detail must be identified with a specific  $S-N$  curve.

The hot spot stress is defined as the fatigue stress at the toe of the weld, where the stress concentration is the highest and where fatigue cracking is likely to initiate (Mansour et al. 1996). The hot spot stress is comprised of membrane and bending stress components, which are linearly distributed over the plate thickness. The hot spot stress analysis takes into account two factors (Moan and Berge 1997): (1) the local increase in membrane stress due to complex structural geometry of welded joint and (2) the information of bending stress due to eccentricity. The exact weld toe geometry and nonlinear stress peak due to local notch at the weld toe are disregarded.

The hot spot stress is an average nominal stress of the stresses near the weld. The advantage of the hot spot stress method is that only one universal  $S$ - $N$  curve is required to define fatigue strength for all welds, if such a curve exists. The disadvantage is that this approach requires detailed finite element analysis to determine the hot spot stress.

## 2.4 Miner's Rule and the Equivalent Stress Range Concept

According to White and Ayyub (1987), the Miner's cumulative damage hypothesis (Miner 1945) is based on the concept of strain energy. The concept of strain energy states that failure occurs when the total strain energy due to  $n$  cycles of variable amplitude loading is equal to the total strain energy from  $N$  cycles of constant amplitude loading. Hence, fatigue damage (or damage ratio) can be written as

$$D = \sum_{i=1}^{n_b} \frac{n_i}{N_i} \quad (6)$$

where  $n_i$  = number of constant amplitude range  $S_i$  stress cycles in block  $i$ ,  $N_i$  = number of cycles to failure at constant stress range  $S_i$ , and  $n_b$  = number of stress blocks. The fatigue damage ratio  $D$  theoretically equals 1.0 at failure, however in practice, because of various uncertainties regarding loads, fabrication, operation, and other modeling errors, the value of  $D$  is usually made less than one.

In most applications, even though the  $S$ - $N$  curves are based on constant amplitude stress cycles, service loadings in most real marine structures are random variables which can be described by probability density functions  $f_S(s_i)$  as shown in Figure 7. The probabilistic characteristics of the variable  $S$  are obtained from recorded stress histories or estimated from wave records and anticipated structural response. The results are usually expressed as a probability density function (PDF) as illustrated in Figure 7. In order to use the  $S$ - $N$  fatigue test data, it is necessary to find a relationship between the characteristic value of the wave-induced random stress and the constant amplitude stress of the  $S$ - $N$  curves. This can be accomplished by applying Miner's principle to find an equivalent stress range  $S_e$ . An expression for  $S_e$  can be found by dividing the random load distribution into a large number of narrow stress blocks of width  $\Delta S$  (Figure 7). In each block, the fractional number of cycles is  $f_S(s_i) \Delta S$ . If  $N$  denotes the

total number of cycles in the life of a structural component of a ship, then the number of cycles in the stress block is given by

$$n_i = Nf_s(s_i)\Delta S \quad (7)$$

Substituting the above equation and Eq. 4 into the Miner's rule equation (Eq. 6), results in

$$D = \sum_{i=1}^{n_b} \frac{Nf_s(s_i)\Delta S}{\frac{A}{S_i^m}} \quad (8)$$

As  $\Delta S$  goes to zero and noting that both  $N$  and  $A$  are constant parameters, Eq. 8 can be put in an integral form as

$$D = \frac{N}{A} \int_0^{\infty} S^m f_s(s) ds \quad (9)$$

where  $f_s(s)$  = stress probability density function. The integral expression of Eq. 9 is the mean or the expected value,  $E(S^m)$ , of the random variable  $S^m$ . Accordingly, the damage ratio  $D$  takes the following form:

$$D = \frac{N}{A} E(S^m) \quad (10)$$

where

$$E(S^m) = \int_0^{\infty} S^m f_s(s) ds \quad (11)$$

The expected (mean) value of Eq. 11 is relatively easily found for a known distribution. For example, the lognormal distribution has a closed-form expression for  $E(S^m)$  as

$$E(S^m) = \mu_s^m \exp \left[ \frac{1}{2} (m^2 - m) \ln \left( \frac{\sigma_s^2}{\mu_s^2} + 1 \right) \right] \quad (12)$$

where  $\mu_s$  and  $\sigma_s$  are the mean and standard deviation of the stress variable  $S$ , respectively. For other probability distributions, expressions for  $E(S^m)$  are found in Table 2. Relationships between the mean and standard deviation of the stress range  $S$  and the characteristic parameters of commonly used probability distributions are provided in Table 3 (Munse et al. 1983). This

table also gives the probability density function (PDF) for these distributions. The shapes of the probability density functions are summarized in Figure 8.

Combining the constant amplitude stress range of the  $S$ - $N$  curve of Eq. 4 and the fatigue damage ratio of Eq. 10, the following expression for an equivalent constant stress range ( $S_e$ ) as a function of fatigue damage is obtained:

$$S_e = m \sqrt[m]{\frac{1}{D} E(S^m)} \quad (13)$$

Theoretically, the fatigue damage ratio  $D$  is equal to unity at failure. However, as mentioned earlier, because of the various uncertainties with regard to loads, operation, fabrication, the value for  $D$  is made substantially less than one by various classification agencies. For example, in offshore structures, the nominal value for  $D$  ranges from 0.1 to 0.3 (DnV 1977).

In the reliability-based fatigue design approach, fatigue failure is assumed to occur when the linear cumulative damage  $D$  of Miner's rule is equal to unity. However, because of the inherent high uncertainties associated with this random variable, the probabilistic characteristics of this random variable ( $D$ ) are needed. In an attempt to investigate the fatigue design process in the welded joints of steel used in offshore structures, Wirsching (1984) recommended a lognormal distribution for the random variable  $D$  with a mean and  $COV$  equal to 1.0 and 0.3, respectively. He asserted that the lognormal distribution for  $D$  has been shown to provide a good fit to the data that were used. If  $D$  is assumed equal to one, as is often the case in most applications, then Eq. 13 can be reduced to the following expression for the equivalent constant amplitude stress  $S_e$ :

$$S_e = m \sqrt[m]{E(S^m)} \quad (14)$$

where  $E(S^m)$  as given by Eq. 11. However, in reliability-based design and analysis approaches, the uncertainty in the linear cumulative damage  $D$  of Miner's rule cannot be ignored.

## 2.5 Performance Functions for Fatigue

As was mentioned earlier, reliability-based analysis and design procedures start with defining performance functions that correspond to limit states for significant failure modes (Mansour et al. 1996). In general, the problem can be considered as one of supply and demand.

Failure occurs when the supply (i.e., strength of the system) is less than the demand (i.e., loading on the system). A generalized form for the performance function for a structural system is given by

$$g_1 = R - L \quad (15)$$

where  $g_1$  = performance function,  $R$  = strength (resistance) and  $L$  = loading in the structure. The failure in this case is defined in the region where  $g_1$  is less than zero or  $R$  is less than  $L$ , that is

$$g_1 < 0.0 \text{ or } R < L \quad (16)$$

As an alternative approach to Eq. 15, the performance function can also be given as

$$g_2 = \frac{R}{L} \quad (17)$$

where, in this case, the failure is defined in the region where  $g_2$  is less than one or  $R$  is less than  $L$ , that is

$$g_2 < 1.0 \text{ or } R < L \quad (18)$$

If both the strength and load are treated as random variables, then the reliability-based design and analysis can be approached using probabilistic methods. In order to perform a reliability analysis, a mathematical model that relates the strength and load needs to be derived. This relationship is expressed in the form of a limit state or performance function as given by Eq. 15 or Eq. 17. Furthermore, the statistical characteristic of the basic random variables that define the strength and loads must be quantified.

The strength of fatigue details can be expressed in the form of stress-range  $S$  versus number of life cycles  $N$ . The determination of stress ranges requires analyzing a structural component under different loading conditions. The number of loading cycles needs to be determined because it constitutes an important component in reliability analysis.

The performance functions that can be used in reliability analysis for fatigue can take two general forms, life cycle formulation and fatigue damage formulation. Both of these formulations are described in the following two sections.

### 2.5.1 Life Cycle Formulation

In this formulation, the performance function for fatigue reliability analysis takes either one of the following two expressions:

$$g_1 = N - N_t \quad (19)$$

or

$$g_2 = \log(N) - \log(N_t) \quad (20)$$

where  $g_1$  and  $g_2$  = performance functions,  $N$  = number of loading cycles to crack initiation, and  $N_t$  = number of loading cycles expected during the life of a structural detail. Using Miner's rule for cumulative fatigue damage with an effective stress formulation for variable amplitude loading (i.e., Eq. 9), Eq. 19 can be expressed as

$$g_1 = \frac{\Delta A}{\varepsilon' S_e^m} - N_t \quad (21)$$

where  $A$  and  $m$  = the intercept and slope of the  $S$ - $N$  strength model curve for a fatigue detail, respectively,  $\varepsilon'$  = uncertainty in the  $S$ - $N$  relationship,  $\Delta$  = Miner's rule damage at failure, and  $S_e$  = effective stress range for variable amplitude loading for a structural component. The effective stress range  $S_e$  is given by

$$S_e = \sqrt[m]{k_s^m E(S^m)} = \sqrt[m]{k_s^m \sum_{i=1}^{n_b} f_i S_i^m} \quad (22)$$

where  $n_b$  = number of stress blocks in a stress (loading) histogram,  $f_i$  = fraction of cycles in the  $i^{\text{th}}$  stress block,  $S_i$  = stress in the  $i^{\text{th}}$  block, and  $k_s$  = fatigue stress damage factor. Eq. 20 can be put in a base-10 logarithmic form in terms of the fatigue variables to give

$$g_2 = \log(A) + \log(\Delta) - m \log(S_e) + \varepsilon - \log(N_t) \quad (23)$$

where  $\varepsilon = -\log(\varepsilon')$ .

### 2.5.2 Fatigue Damage Ratio Formulation

In this case, the performance function for fatigue reliability analysis for takes either one of the following two expressions:

$$g_1 = \Delta - D \quad (24)$$

or

$$g_2 = \log(\Delta) - \log(D) \quad (25)$$

where  $g_1$  and  $g_2$  = performance functions,  $\Delta$  = random variable denoting fatigue damage at failure, and  $D$  = fatigue damage expected during the life of a structural detail. Again, using Miner's rule for cumulative fatigue damage with an effective stress formulation for variable amplitude loading, Eqs. 24 can be expressed as

$$g_1 = \Delta - \sum_{i=1}^{n_b} \frac{n_i}{N_i} \quad (26a)$$

where  $\Delta$  = fatigue damage ratio limit that has a mean value of one;  $n_i$  = number of actual load cycles at the  $i$ th stress-range level;  $N_i$  = number of load cycles to failure at the  $i$ th stress-range level; and  $n_b$  = number of stress-range levels in a stress range histogram. Eq. 26a can be expressed as

$$g_1 = \Delta_L - \sum_{i=1}^{n_b} \frac{n_i}{A k_S^m S_i^m} \quad (26b)$$

If a lognormal distribution of fatigue failure lives is assumed, probability of failure can be associated with a number of standard deviations from the mean  $S-N$  curve. Using two-standard deviations ( $2\sigma$ ) from a mean regression line that represent the  $S-N$  strength of fatigue detail, Eq. 26b can be expressed as

$$g_1 = \Delta_L - \sum_{i=1}^{n_b} \frac{n_i}{10^{(\log(A) - 2\sigma)} k_S^m S_i^m} \quad (27)$$

where  $A$ ,  $m$ , and  $\sigma$  are obtained from linear regression analysis of  $S-N$  data in a log-log space. Equation 27 can be used to perform reliability analysis and safety checking as provided in Figure 13.

## 2.6 Fatigue Details

Fatigue of ship and offshore structural details is primarily a result of the action of seawater waves (Byers et al. 1997) and the sea environment in general. The load cycles in such an environment can be on the order of million cycles per year. Fatigue failures in ship and offshore structures can take place at sites of high stress concentration that can be classified into two major categories: (1) baseplate and (2) weldments. The former includes locations of high stress concentration such as openings, sharp re-entry corners, and plate edges.

Fatigue behavior of a structural detail is a function of a variety of factors. These factors include but are not limited to: (1) the general configuration and local geometry of the member or detail, (2) the material from which the members are made, (3) welding that is used to produce continuity in the joints and members of a welded structures, and (4) the loading conditions to which the detail is subjected. Some of these factors have relatively little effect, while others have a significant impact and should be included in the design process. Probably the most important factor in fatigue design that has a significant effect on its resistance is the geometry of the member or detail. Figure 9 is an example of the effect of general configuration of two members. The fatigue resistance (strength) of the members shown in the figure differs in magnitude by a factor of 2.5 for the same resistance. This example clearly demonstrates the important role played by the configuration and welded details of the members. The significance of local geometry of weldments can be demonstrated by examining in more detail the fatigue resistance at 2,000,000 cycles of a butt-welded splice of Figure 9a. The butt weld reduces the fatigue strength of the detail to about 56 percent of the unwelded base plate fatigue resistance (Munse et al.1984). The specific magnitude of this reduction is dependent upon the type of steel used, the local configuration of the weld, and a variety of other factors.

Due to the numerous types of structural members found in ship structures, classification of these members is needed to establish their fatigue resistance. The classification of these details is also important for reliability-based fatigue design and assessment of ship structures. This classification can serve to group them based on their geometry, loadings, and similar fatigue resistance and can make possible the establishment of mean fatigue resistance and variability of each different type of member.

As mentioned earlier, the most important factor in fatigue design that has a significant effect on its resistance is the geometry of the member or detail. Because of the large variety of structural details found in modern ships, a great attention in recent years has focused on the classifications of these details. Researchers such as Munse et al. (1983), Jordan (1978), Glasfeld et al. (1977), and others have conducted studies of structural details to help identify those locations in a ship that may be fatigue critical and to establish design criteria for such details. For example, to identify the possible critical locations, Munse et al. (1983) have developed a catalog of ship structural details and assemblies. The ship details included in their investigation are representative of current ship design and ship yard practice. Figure 10 provides a sample for these details as given by Munse et al. (1983), while Table 4 gives mean fatigue strength for a range of fatigue details of Figure 10. A detailed summary of this catalog is provided in Munse et al. (1983) and Assakkaf (1998). Results of additional tests of ship structural details are provided by Kihl (1999).

In general, ship structural details have been developed with little or no fatigue analysis included in the detail selection and design process (Munse et al. 1983). Although there are some basic selection factors used in terms of size and configurations, only limited fatigue design information has been available to the designer or user to help in his selection. The details have often been chosen because they have been used previously or are easy to assemble. Accordingly, a large variety of structural details with great varying fatigue resistance have been noticed. To provide data on the performance of structural details, Jordan and Cochran (1978 and 1980) have conducted a series of studies on ship structures to identify poor details as well as to reduce the number of variations in details and to decrease fabrication and construction costs. Their studies include surveys of actual in-service performance of many of these structural details now in use. In these surveys, the details are divided into twelve categories and cover 634 structural configurations. Eighty-six ships involving seven types were surveyed for service failures. Approximately 600,000 details were identified and 6,856 of these details exhibited failures. These efforts by Jordan and Cochran (1978 and 1980), directed toward the evaluation of ship structural details, have helped a great deal in defining the critical locations in the details.

### 3. DESIGN LOADS

#### 3.1 Spectral Analysis

Spectral analysis is used to develop a lifetime fatigue and extreme loads spectrum by considering the operational conditions of a ship at sea to be divided into different operation modes according to combinations of speeds, headings, and wave heights as shown in Figure 11 (Sikora et al. 1983). The operational mode is defined by the ship speed, heading relative to the sea, and the sea condition. Each operational mode results in a response spectrum (in this case the wave-induced bending moment) which is the product of a wave spectrum and a response amplitude operator (RAO), where the RAO is defined as the response per input wave height squared as a function of wave frequency. Each response spectrum defines a Rayleigh probability distribution of response amplitudes. The total number of cycles included in each distribution is the product of the time spent in that incremental mode and the average encounter frequency of the response spectrum.

The time spent at sea for each operational condition is given by (Sikora et al. 1983)

$$T_i = T_y P_1 P_2 P_3 P_4 \quad (28)$$

where  $T_y$  = life-time at sea;  $P_1$  = ship heading probability;  $P_2$  = ship speed probability;  $P_3$  = wave height probability; and  $P_4$  = wave spectral probability. The average encounter frequency may be determined from the second moment of the response spectrum as given by (Sikora et al. 1983)

$$\omega_{ie} = \sqrt{\frac{\sum_j A_j \omega_{iej}^2}{\sum_j A_j}} \quad (29)$$

where  $A_j$  = area under an increment of the response function,  $\omega_{iej}$  = wave excited frequency of the ship at the  $i$ th mode and the  $j$ -th response function, and  $N_i$  = the number of cycles at the  $i$ th mode and is given by (Sikora et al. 1983)

$$N_i = \frac{T_i \omega_{ie}}{2\pi} \quad (30)$$

The number of response cycles exceeding any response magnitude was determined from the area under a portion of the Rayleigh distribution of the response magnitude. The maximum lifetime amplitude load for each response function is obtained from Eq. 31 (Sikora et al. 1983)

$$F_{i_{max}} = \sqrt{E_i \ln N_i} \quad (31)$$

Where  $F_{i_{max}}$  = maximum lifetime amplitude load for each response function, and  $E_i$  = the mean squared amplitude of the response function (twice the area under the curve of the  $i^{\text{th}}$  response spectrum). This value is expected to be exceeded once during that particular operational mode, i.e., area under the tail of the Rayleigh distribution corresponds to one cycle. Hence, the single maximum lifetime load expected to be exceeded once during its lifetime of the ship can be found using the following equation (Sikora et al. 1983):

$$\sum_{j=1}^{N_m} \exp\left[\frac{-F_{max}^2}{E_i}\right] N_i = 1.0 \quad (32)$$

where  $N_m$  = number of operation modes, and  $F_{max}$  = the single lifetime maximum load expected once in the ship's lifetime. This value is such that the sum of the areas under the tails of all Rayleigh distributions for all the operational modes (fraction of cycles) constitute to one complete cycle. Sikora et al. (1983) used the six-parameter family of spectra presented by Ochi (1977, 1978) to present the sea in this study. However all the basic random variables that affect the wave load effects were considered to be deterministic values.

A lifetime fatigue exceedance curve can be obtained using Eq. 32 by replacing  $F_{max}$  with the desired value of the load and calculating the corresponding number of cycles, which equals or exceeds the specified response. Contributions from bow slamming and whipping of the ship hull can also be incorporated into the lifetime fatigue exceedance curve (Sikora et al. 1983).

### 3.2 Bending Moment and Stress Spectra

Sikora et al (1983) uses the six-parameter family of spectra presented by Ochi et al. (1977) and Ochi (1978) to represent the sea environment in which a ship operates. All the basic random variables that have an effect on the wave loads are considered to be deterministic. It is possible to obtain a lifetime fatigue exceedance curve using Eq. 32 by replacing  $F_{max}$  with the desired value of the load and computing the corresponding number of cycles, which equals or exceeds the specified response. The exceedance curve can then be converted to histogram plot for subsequent fatigue analysis. Table 5 shows a typical histogram (moment or stress range vs. cycles) established for a ship.

In an effort to investigate the uncertainties associated with the wave loads on cruisers, Ayyub and Atua (1996) utilized the SPECTRA program (Sikora 1983) to generate bending moment histograms. The output of their work is shown in Tables 6 and 7. These tables summarize the wave bending moment spectra in both sagging and hogging conditions based on the number of occurrence of each value of the wave load during the lifetime of the ship. Table 6 gives a sample wave-induced bending moment spectra while Table 7 provides a sample spectra for the combined wave-induced and whipping bending moment.

The response spectra such as those found in Tables 6 and 7 for the bending moments are essential for direct reliability assessment and design for fatigue. However, in order for these spectra to be useful, the units are usually converted to stress by dividing these moments by the hull section modulus amidships. The stress response at locations other than the strength deck can be determined by using stress transfer factors to adjust the stress (White 1992). Stress concentrations due to component geometry can be handled in a similar fashion. Table 8 shows typical values of hull section modulus  $Z$  for different classes of destroyer type of naval ships (Sikora et al. 1983). Table 8 also shows the particulars of these ships (i.e., LBP, Beam, depth, etc.). Once a histogram of stress range versus life cycles is established for a particular ship, the equivalent stress range  $S_e$  can be computed according to the following equation:

$$S_e = \sqrt[m]{\sum_{i=1}^{n_b} f_i S_i^m} \quad (33)$$

where  $m$  = slope of the  $S-N$  curve,  $S_i$  = stress in the  $i^{\text{th}}$  block,  $f_i$  = fraction of cycles in the  $i^{\text{th}}$  block, and  $n_b$  = number of stress blocks in a stress (loading) histogram. The equivalent stress range, as given by Eq. 33, is crucial for direct reliability-based design and analysis for fatigue.

Figure 12 provides a schematic for the procedures involved for producing a moment response histogram as well as stress response histogram. However, sometimes a load probability distribution for moment or stress is available and can be used directly.

## **4. RELIABILITY-BASED DESIGN GUIDELINES FOR FATIGUE**

### **4.1 Target Reliability Levels**

Selecting a target reliability level is required in order to establish reliability-based design guidelines for ship structures such as the hull girder. The selected reliability level determines the probability of failure of the structural detail. The following three methods can be used to select a target reliability value:

1. Agreeing upon a reasonable value in cases of novel structures without prior history.
2. Calibrating reliability levels implied in currently used design codes.
3. Choosing a target reliability level that minimizes total expected costs over the service life of the structure for dealing with design for which failures result in only economic losses and consequences.

The recommended range of target reliability indices for fatigue can be set to range from 2.0 to 4.0 (Mansour et al. 1996).

### **4.2 Statistical Characteristics of Fatigue Random Variables**

#### **4.2.1 Uncertainty in Fatigue Strength**

Uncertainty in fatigue strength is evidenced by the large scatter in fatigue  $S-N$  data. The scatter of the data about the mean fatigue line is not the only uncertainty involved in fatigue analysis (Ayyub and White 1987). For this reason, a measure of the total uncertainty in the form of a coefficient of variation ( $COV$ ) in fatigue life is usually developed to include the uncertainty

in data, errors in fatigue model, and any uncertainty in the individual stresses and stress effects. According to Ang and Munse (1975), the total coefficient of variation (*COV*) in terms of fatigue life can be given by

$$\delta_N = \sqrt{\delta_f^2 + \delta_A^2 + m^2 \delta_S^2} \quad (34)$$

where  $\delta_N$  = total *COV* in terms of cycles to failure,  $\delta_f$  = variation (*COV*) due to errors in fatigue model and utilization of Miner's rule,  $\delta_A$  = uncertainty (*COV*) in mean intercept of the regression line including effects of fabrication, workmanship, and uncertainty in slope,  $\delta_S$  = uncertainty (*COV*) in equivalent stress range including effects of error in stress analysis, and  $m$  = slope of mean *S-N* regression line. Values for  $\delta_N$  and  $m$  are obtainable from sets of *S-N* curves for the type of detail under consideration. Munse et al. (1983) has managed to tabulate such values. Typical values for  $\delta_S$ ,  $\delta_A$ , and  $\delta_f$  are 0.1, 0.4, and 0.15, respectively.

Other researchers such as Wirsching (1984) and Ayyub et al. (1998) have approached the same source of uncertainty in a slightly different way. For example, Wirsching (1984) introduces the random variable  $B$  to represent a bias factor and the random variable  $\Delta$  to denote fatigue damage at failure. The bias factor  $B$  is assumed to account for the stress modeling error, while the fatigue damage at failure  $\Delta$  is to quantify the modeling error associated with Miner's rule, which is presented in the next section. He also suggests that uncertainty in fatigue strength can be accounted for by considering the intercept of the *S-N* curve ( $A$ ) as a random variable with the slope of the same *S-N* curve ( $m$ ) taken as a constant. Uncertainty in  $B$ , as described by Wirsching (1984), is assumed to stem from five sources: (1) fabrication and assembly operations, (2) sea state description, (3) wave load prediction, (4) nominal member loads, and (5) estimation of hot spot stress concentration factor.

Ayyub et al. (1998), in assessing the fatigue reliability of miter gates components for the U.S. Army Corps of Engineers (USACE), chose to look at the same sources of uncertainty in a slightly different way. He introduces the random variables  $\varepsilon'$  and  $k_s$  to account respectively for the uncertainty in the *S-N* relationship and fatigue stresses. The author also uses a factor  $\Delta$  similar to that of Wirsching (1984) to account for the uncertainty due to the utilization of linear cumulative damage of Miner's rule. A full coverage of fatigue parameter uncertainties is presented in Munse et al. (1983) and Assakkaf (1998).

## 4.2.2 Fatigue Details and Data

Characteristic  $S-N$  curves are available in different design codes for various structural details in bridges, ships, and offshore structures. In these curves, the mean value of fatigue life for a given stress range is usually reduced by two standard deviations to account for scatter in the  $S-N$  data. This implies a finite probability of failure for a known stress range, which is about 2.3%, assuming  $N$  has a lognormal distribution. The actual probabilities of failure associated with fatigue design lives can be higher due to uncertainties associated with:

1. calculated stresses,
2. the various correction factors on the  $S-N$  curves, and
3. the critical value of the cumulative fatigue damage,  $\Delta$ .

This section provides a summary of statistical data for fatigue random variables of ship structural details. This summary includes data of the joint classification for British Standards (BS 5400) and the DnV (1977). A sample fatigue detail is provided as shown in Figure 8. Additional details are provided by Sieve, et al. (2000).

### 4.2.2.1 British Standards and DnV Structural Details

Table 9 provides description of joint classes for fatigue based on both the British standards (1980) and the DnV specifications (1977). Table 10 provides statistical information for fatigue variables of these details.

### 4.2.2.2 Statistical Data on Fatigue Details as Given by Munse et al. (1983)

The measure of total uncertainties ( $COV$ 's) in fatigue life  $\delta_N$  is given by

$$\delta_N = \sqrt{\delta_f^2 + \delta_A^2 + m^2 \delta_S^2} \quad (35)$$

where

$\delta_N$  = total uncertainty ( $COV$ ) in terms of cycles to failure

$\delta_f$  = variation ( $COV$ ) due to errors in fatigue model and use of Miner's rule

$\delta_A$  = uncertainty ( $COV$ ) in mean intercept of the regression line including effects of fabrication, workmanship, and uncertainty in slope

$\delta_S$  = uncertainty ( $COV$ ) in equivalent stress range including effects of error in stress analysis

$m$  = slope of mean  $S-N$  regression line

The uncertainty (*COV*) in  $\delta_f$  comes from two sources: uncertainty in fatigue data about the *S-N* regression line  $\delta_{S-N}$  and the uncertainty due to the utilization of Miner's rule  $\delta_M$ . The *COV* of  $\delta_f$  is given by

$$\delta_f = \sqrt{\delta_{S-N}^2 + \delta_M^2} \quad (36)$$

Quantification of above different sources of uncertainties is tabulated as provided by different sources such as Munse et al. (1983) and Assakkaf (1998).

#### **4.2.2.3 Statistical Information on Fatigue Damage Ratio *D***

Statistical data on fatigue damage ratio is provided in Wirsching and Chen (1988) and White (1992) as shown in Table 11. Table 12 provides ranges for the median and *COV* of  $\Delta$ . The range values given in Table 12 are based on the statistical information provided in Table 11.

### **4.3 Sample LRFD Guidelines**

Reliability-based design for fatigue of ship structural details can be performed according to the subsequent sections. It can be either as a direct reliability-based design or using the load and resistance factor design (LRFD) format. Recent Navy design guidance for fatigue that includes reliability-based design is described by Sieve, et al. (2000).

#### **4.3.1 Direct Reliability-Based Design**

##### **4.3.1.1 Direct Reliability-Based Design Method**

A direct reliability-based design requires performing spectral analysis for the loads. The spectral analysis shall be used to develop lifetime fatigue loads spectra by considering the operational conditions and the characteristics of a ship at sea. The operational conditions are divided into different operation modes according to the combinations of ship speeds, ship headings, and wave heights. The ship characteristics include the length between perpendicular (*LBP*), beam (*B*), and the bow form as shown in Figure 13. With the proper identification of the hull girder section modulus (*Z*), the bending moment histograms (moment range versus number of cycles) can be converted to mean stress range spectra to compute the equivalent stress range  $\bar{S}_e$  according to the following equation

$$\bar{S}_e = \sqrt[m]{\sum_{i=1}^{n_b} f_i S_i^m} \quad (37)$$

where  $\bar{S}_e$  = Miner's mean equivalent stress range;  $S_i$  = stress in the  $i^{\text{th}}$  block;  $f_i$  = fraction of cycles in the  $i^{\text{th}}$  stress block;  $m$  = slope of  $S$ - $N$  curve; and  $n_b$  = number of stress blocks in a stress (loading) histogram. The direct reliability-based design for fatigue requires the probabilistic characteristics of the random variables in the performance function equation. It also requires specifying a target reliability index  $\beta_0$  to be compared with a computed  $\beta$  resulting from reliability assessment methods such as the first-order reliability method (FORM). The general form for reliability checking used in the guidelines is given by

$$\beta \geq \beta_0 \quad (38)$$

#### 4.3.1.2 Reliability Checking for Fatigue

To perform a reliability check on fatigue design for a ship structural detail, the computed reliability safety index  $\beta$  resulting from reliability assessment using for example FORM should not be less than the target safety index  $\beta_0$  as given by Eq. 38. The following steps can be followed to perform reliability checking on an existing ship structural fatigue detail (see Figure 13):

1. For given ship characteristics (i.e., LBP, Beam, hull section modulus, etc.), operational profiles (i.e., speed, heading), ship lifetime at sea, and area of operation, generate stress range spectra using for example the program SPECTRA.
2. With the generation of stress range spectra, estimate the mean equivalent stress range using Eq. 36.
3. Select a target reliability index  $\beta_0$ , a ship structural detail, and design life, e.g., a vessel life of 25 years.
4. Assign probabilistic characteristics to the fatigue variables ( $\Delta$ ,  $A$ ,  $k_s$ ) in the performance function of equation Eq. 27. Also, the  $COV$  of  $\bar{S}_e$  and its distribution type should be determined in this step.
5. Once all the variables are identified and computed in steps 1 through 4, use reliability methods such as FORM to compute the safety (reliability) index  $\beta$ .

The reliability or safety index  $\beta$  computed in step 5 is compared with the target reliability index  $\beta_0$  as given by Eq. 38. If  $\beta$  is equal to or greater than  $\beta_0$ , this means that the structural detail under study is adequate, otherwise change member size, cross section, or fatigue detail (i.e., joint) and repeat steps 3 to 6.

#### 4.3.1.3 Computation of Reliability-based Design Stress

In order to compute the design stress for a ship structural detail, the following steps can be followed:

1. Select a target reliability index  $\beta_0$  and a ship structural detail.
2. Assign probabilistic characteristics to the fatigue variables ( $\Delta, A, k_s$ ) in the performance function equation (Eq. 27).
3. For the selected target reliability index  $\beta_0$ , probability distributions and statistics (means  $COV$ 's) of the fatigue variables ( $\Delta, A, k_s$ ), and the coefficient of variation of the stress range  $S_e$ , compute the mean value of  $S_e$  (i.e.,  $\bar{S}_e$ ) using reliability methods such as FORM. The mean stress value ( $\bar{S}_e$ ) is the design stress.
4. Develop a joint geometry that results in a mean stress less than the mean stress value ( $\bar{S}_e$ ) of step 3.

#### 4.3.2 Load and Resistance Factor Design

An alternative approach for reliability-based design is the use of partial safety factors (PSF's) using a load and resistance factor (LRFD) design format. The PSF's are defined for both strength and load variables. They are commonly termed strength reduction and load amplification factors. The structural detail or joint element of a ship should meet one of the following performance functions:

$$\gamma_{S_e} S_e \leq \left[ \frac{n_i}{\phi_A A \gamma_{k_s}^m k_s^m \phi_{\Delta} \Delta} \right]^{\frac{1}{m}} \quad (39)$$

where

$$S_e = \sqrt[m]{\sum_{i=1}^{n_b} f_i S_i^m} \quad (40)$$

and  $S_e$  = Miner's equivalent stress range;  $\phi_\Delta$  = reduction safety factor corresponds to fatigue damage ratio  $\Delta$ ;  $\phi_A$  = reduction safety factor corresponds to the intercept of the  $S$ - $N$  curve;  $\gamma_{k_s}$  = amplification safety factor for fatigue stress uncertainty; and  $\gamma_{S_e}$  = amplification safety factor for Miner's rule equivalent stress range.

It is to be noted that the nominal equivalent stress,  $S_e$ , is the best estimate resulting from spectral analysis. The nominal (i.e., design) values of the fatigue variables should satisfy these formats in order to achieve specified target reliability levels.

The probabilistic characteristics and nominal values for the strength and load components were determined based on statistical analysis, recommended values from other specifications, and by professional judgment. These factors are determined using structural reliability methods based on the probabilistic characteristics of the basic random variables for fatigue including statistical and modeling (or prediction) uncertainties. The factors are determined to meet target reliability levels that were selected based on assessing previous designs. This process of developing reliability-based LRFD guidelines based on implicit reliability levels in current practices is called code calibration.

The LRFD design for fatigue, as given in Eq. 39, requires partial safety factors and nominal values. The partial safety factors (PSF's) are provided in Tables 13 and 14 according to the following requirements:

1. Target reliability levels in the range from 2.0 to 4.0,
2. Fatigue strength prediction methods based on Miner's linear cumulative damage theory and on the characteristic  $S$ - $N$  curve, and
3. Selected details of the British standards (BS 5400).

A target reliability level should be selected based on the ship class and usage. Then, the corresponding partial safety factors can be looked up from Tables 13 and 14 based on the appropriate detail for joint for selected details. Similar tables can be developed for other details.

## 5. DESIGN EXAMPLE

In this example, a direct reliability-based procedure is used. This procedure is used to perform safety checking by evaluating the reliability indices based on selected pairs of  $m$  and  $A$  that correspond to certain fatigue details of interest, and identifying the details that meet or exceed the specified target reliability of 2.5. The performance function as defined in Eq. 27 is used in this example, where  $\Delta$ ,  $A$ ,  $k_s$ , and  $S_e$  are random variables. The probabilistic characteristics of the random variables that are used for each detail in this example are provided in Tables 15 through 18. Summaries of the results based on this approach are shown in Table 19.

An alternative procedure is to determine the design stress (mean of  $S_e$ ) for each detail as previously outlined. For target reliability  $\beta_0$  of 2.5, probabilistic distributions and statistics of fatigue random variables for each detail, and the coefficient of variation of  $S_e$ , the mean design stress can be evaluated for each detail. The results based on this approach are summarized in Table 20.

## 6. SUMMARY AND CONCLUSIONS

Future design guidelines for fatigue of ship structures will be developed using reliability methods, and can be expressed as either direct reliability-based design or in a load and resistance factor design (LRFD) format. Marine and offshore structures are subjected to fatigue primarily due to the action of ocean waves and the sea environment in general. The load cycles in such an environment can be on the order of a million cycles per year. Fatigue failures in these structures can take place at sites of high stress concentration that can be classified into two major categories: baseplate and weldments. The former includes locations of high stress concentration such as openings, sharp re-entry corners, and plate edges. In general, the mechanisms behind these failures are described by the general approaches to fatigue life prediction as discussed in this paper. There are two major approaches for evaluating fatigue life prediction: (1) the  $S-N$  curves approach and (2) the fracture mechanics (FM) approach. The  $S-N$  curve approach is based on experimental measurement of fatigue life in terms of cycles to failure for different loading levels, while the fracture mechanics (FM) approach is based on the existence of an initial crack and subsequent growth and propagation under service loads.

This paper presented the developments of reliability-based design methods for fatigue of structural details for conventional displacement type surface monohull ships. These developments are based on the  $S-N$  approach and on the assumption that fatigue damage accumulation is a linear phenomenon (Miner's rule). The methods are also based on structural reliability theory and can be applied either as a direct reliability-based design or in a load and resistance factor design (LRFD) format. The resulting design methods are referred to as an LRFD approach for fatigue of ship structures. These design methods were developed according to the following requirements: (1) spectral analysis of wave loads, (2) building on conventional codes, (3) nominal strength and load values, and (4) achieving target reliability levels. The first-order reliability method (FORM) was used to develop the partial safety factors (PSF's) for selected fatigue limit state equations and for demonstration purposes.

## **ACKNOWLEDGMENTS**

The authors would like to acknowledge the opportunity and support provided by the Carderock Division of the Naval Surface Warfare Center of the U.S. Navy through its engineers and researchers that include J. Adamchak, J. Beach, T. Brady, D. Bruchman, J. Conley, J. Dalzell, A. Disenbacher, A. Engle, W. Hay, P. Hess, R. Lewis, W. Melton, and W. Richardson; and the guidance of the Naval Sea System and Command by E. Comstock, J. Hough, R. McCarthy, N. Nappi, T. Packard, J. Snyder, and R. Walz.

## **REFERENCES**

1. Ang, A. H-S. and Munse, W. H., 1975. "Practical Reliability Basis for Structural Fatigue," Meeting Reprint 2492, ASCE, National Structural Engineering Conference.
2. Assakkaf, I. A., 1998. "Reliability-based Design of Panels and Fatigue Details of Ship Structures," A dissertation submitted to the Faculty of the Graduate School of the University of Maryland, College Park in partial fulfillment of the requirements for the degree of Doctor of Philosophy.
3. Ayyub, B. M. and White, A. M., 1987. "Reliability-Conditioned Partial Safety Factors", Journal of Structural Engineering, Vol. 113, No. 2, February, ASCE, 280-283.

4. Ayyub, B.M. and Atua, K., 1996, LRFD Rules for Naval Surface Ship Structures, Part I: Hull Girder Bending, Naval Surface Warfare Center, Bethesda, MD.
5. Ayyub, B.M., Assakkaf, I., Atua, K., Engle, A., Hess, P., Karaszewski, Z., Kihl, D., Melton, W., Sielski, R.A., Sieve, M., Waldman, J., and White, G. J. 1998. "Reliability-based Design of Ship Structures: Current Practice and Emerging Technologies," Research Report to the US Coast Guard, SNAME, T & R Report R-53.
6. Beer, F. P., and Johnston, E. R., 1981. "Mechanics of Materials," McCraw-Hill, Inc., 41-42.
7. Broek, D., 1986. "Elementary Engineering Fracture Mechanics." 4th Edition, Martinus Nijhoff Publishers, Dordrecht, The Netherlands.
8. BS 5400 (British Standards), 1980. "Steel, Concrete, and Composite Bridges; Code of Practice for Fatigue."
9. Byars, E. F., and Snyder, R. D., 1975. "Engineering Mechanics of Deformable Bodies," Third Edition, Thomas Y. Crowell Company Inc., 427-430.
10. Byers, W. G., Marley, M. J., Mohammadi, J., Nielsen, R. J., and Sarkani, S., 1997. "Fatigue Reliability Reassessment Procedures: State-OF- The-Art Paper." Journal of Structural.
11. Ditlevsen, O., 1986. "Random Fatigue Crack Growth – a first-passage problem." Engineering Fracture Mechanics, 23, 467-477.
12. DnV, 1977. "Specifications for Ships, Det Noreske Veritas, 1322, Hovik, Norway.
13. Glasfeld, R., Jordan, D., Ken, M., Jr., and Zoller, D., 1977. "Review of Ship Structures Details." SSC-266.
14. Harris, D. O., 1995. "Probabilistic Fracture Mechanics." Probabilistic Fracture Mechanics handbook, Sundarajan, ed., Chapman and Hall, New York, N.Y.
15. Hughes, O. F., 1988. "Ship Structural Design, A rationally-Based, Computer-Aided Optimization Approach," The Society of Naval Architects and Marine Engineers, Jersey City, New Jersey.
16. International Institute of Welding (IIW), 1996. "Recommendations on Fatigue of Welded Components," Abington Publishing, Cambridge.
17. Jordan, C. R. and Cochran, C. S., 1978. "In-Service Performance of Structural Details," SSC-272.
18. Jordan, C. R. and Cochran, C. S., 1980. "Further Survey of In-Service Performance of Structural Details," SSC-294.

19. Kihl, D. P., 1999. "Fatigue Strength and Behavior of Ship Structural Details," NSWCCD-65-TR-1998/23.
20. Lin, Y. K., and Yang, J. N., 1983. "On Statistical Moments of Fatigue Crack Propagation." *Engrg. Fracture Mechanics*, 18(2), 243-256.
21. Madsen, H. O., 1983. "Probabilistic and Deterministic Models for Predicting Damage Accumulation due to Time Varying Loading." *DIALOG 5-82*, Danish Engrg., Acad., Lyngby, Denmark.
22. Mansour, A. E., Jan, H. Y., Zigelman, C. I., Chen, Y. N., Harding, S. J., 1984. "Implementation of Reliability Methods to Marine Structures," *Trans. Society of Naval Architects and Marine Engineers*, Vol. 92, 11-20.
23. Mansour, A.E., Wirsching, P.H., and White, G.J., and Ayyub, B. M., 1996. "Probability-Based Ship Design: Implementation of Design Guidelines," SSC 392, NTIS, Washington, D.C., 200 pages.
24. Miner, M. A., 1945. "Cumulative Damage in Fatigue," *Trans. ASME*, 67, *Journal of Applied Mechanics*, 12, 154-164.
25. Moan, T. and Berge, S., 1997. "Fatigue and Fracture," Committee III.2, Proceedings of the 13th International Ship and Offshore Structures Congress, Norwegian University of Science and Technology, Trondheim, Norway, 292-294.
26. Munse, W. H., Wilbur, T. W., Tellalian, M. L., Nicoll, K., and Wilson, K., 1983. "Fatigue Characterization of Fabricated Ship Details for Design," SSC-318, Washington, D.C.
27. Niemi, E., 1995. "Stress Determination for Fatigue Analysis of Welded Components," Abington Publishing, Cambridge.
28. Ochi, M. and Bales, S., 1977, "Effect of Various Spectral Formulations in Predicting Responses of Marine Vehicles and Ocean Structures," presented at the 9th Annual OTC in Houston, Texas.
29. Ochi, M., 1978, "Wave Statistics for the Design of Ships and Ocean Structures," presented at the Annual Meeting of SNAME, NY.
30. Ortiz, K., 1985. "On the Stochastic Modeling of Fatigue Crack Growth," PhD dissertation, Stanford University, Stanford, California.

31. Sieve, M. W., Kihl, D. P., and Ayyub, B. M., Fatigue Design Guidance for Surface Ships, Technical Report NSWCCD-65-TR-2000/25, Naval Surface Warfare Center, U. S. Navy, 2000.
32. Sikora, J. P., Dinsenbacher, A., and Beach, J. A., 1983. "A Method for Estimating Lifetime Loads and Fatigue Lives for Swath and Conventional Monohull Ships," Naval Engineers Journal, ASNE, 63-85.
33. University of Tennessee, Welding Research and Engineering, 1985. "Bibliography on Fatigue of Welds," Research Report.
34. White, G. and Ayyub B., 1987. "Reliability-Based Fatigue Design for Ship Structures," Naval Engineers Journal, May.
35. White, G. J., 1992. "Fatigue of Ship Structural Details: A Probabilistic Approach for Design," U.S. Naval Academy, Annapolis, Maryland.
36. Wirsching, P. H. and Chen, Y. N., 1988. "Considerations of Probability Based Fatigue Design Criteria for Marine Structures," Marine Structures, Vol. 1, 23-45
37. Wirsching, P. H., 1984. "Fatigue Reliability for Offshore Structures." Journal of Structural Engineering, Vol. 110, No. 10, Paper No. 19235, ASCE.

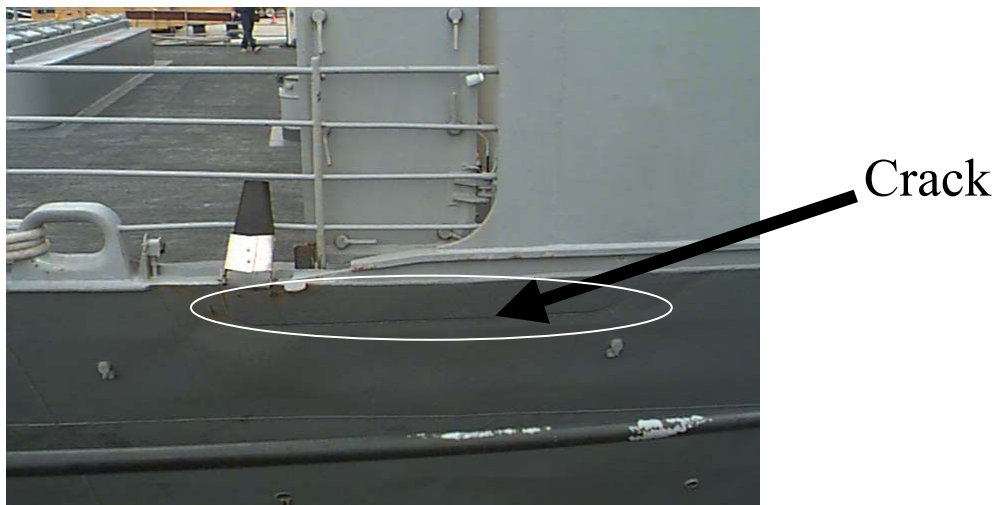


Figure 1. Crack Initiation in Ship due to Fatigue



Figure 2. Crack Propagation

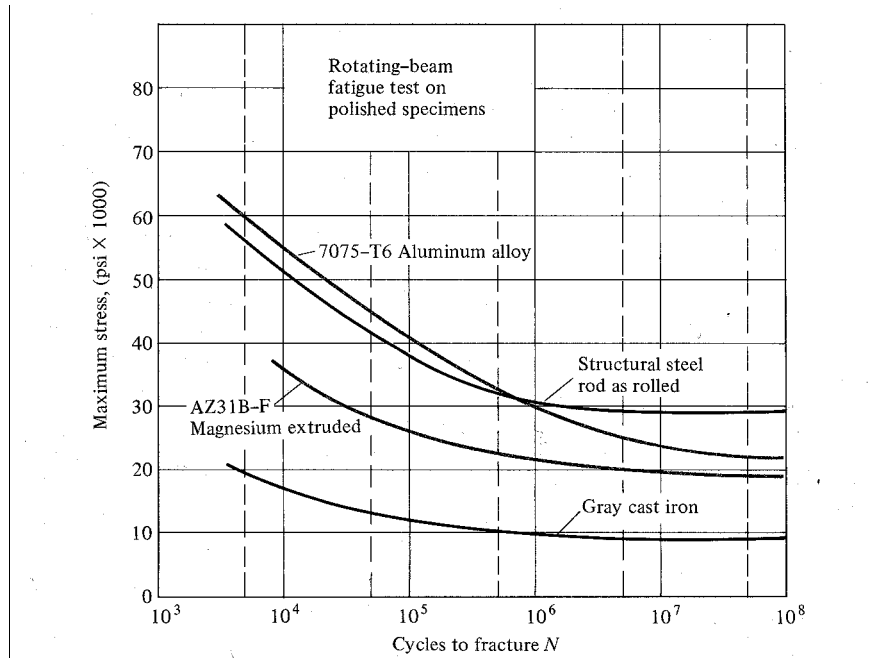


Figure 3. *S-N* Curves for Various Materials (Byars and Snyder, 1975)

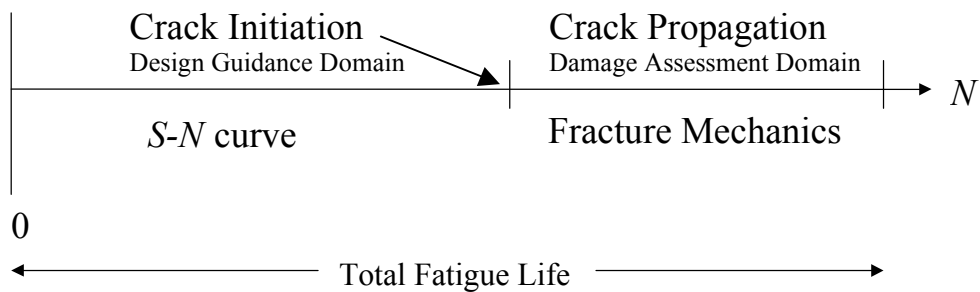


Figure 4. Comparison between the Characteristic *S-N* curve and Fracture Mechanics Approach

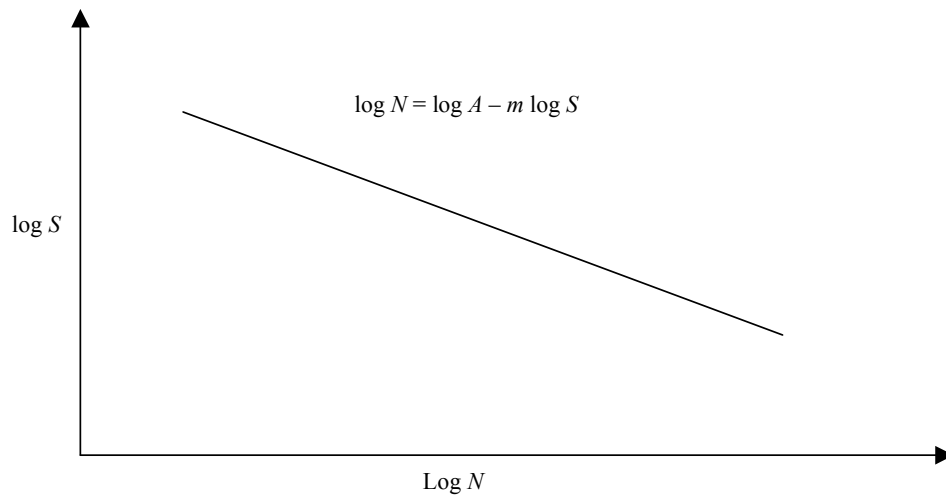


Figure 5. *S-N* Relationship for Fatigue

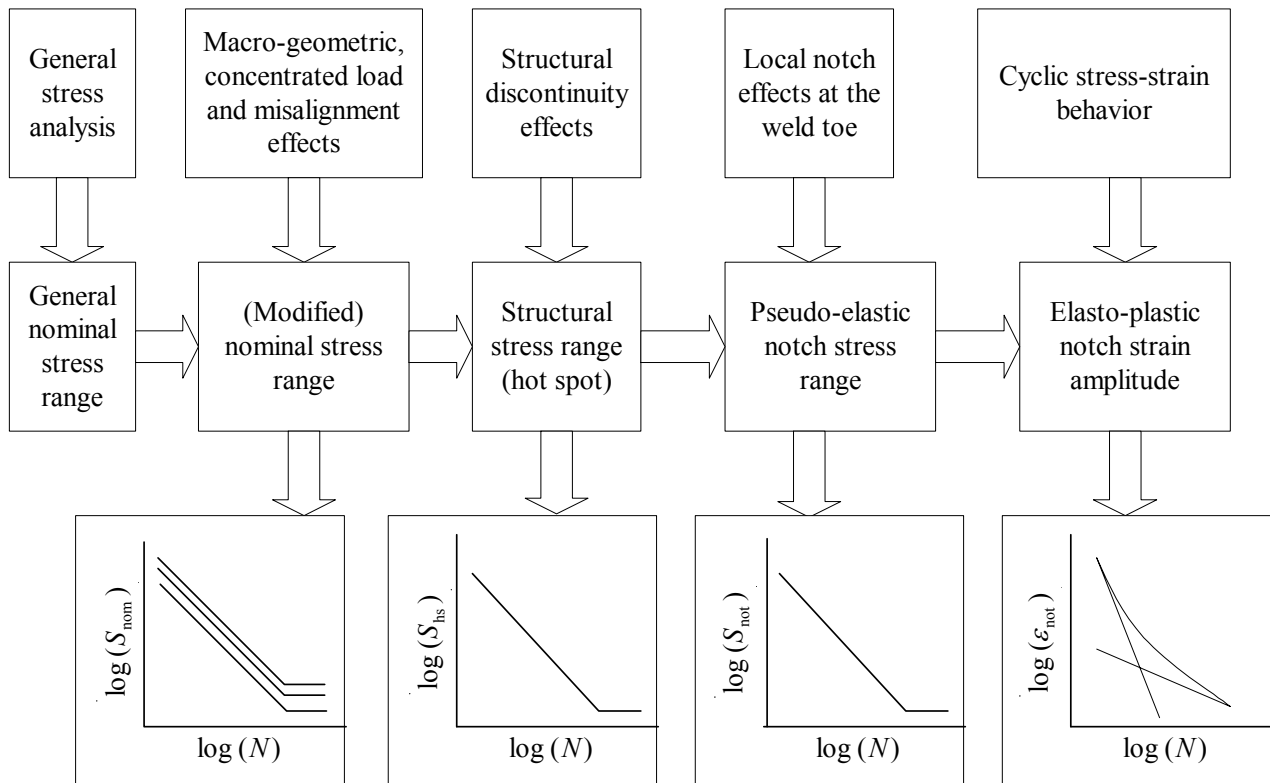


Figure 6. *S-N* Approaches for Fatigue Strength Assessment (Niemi 1995)

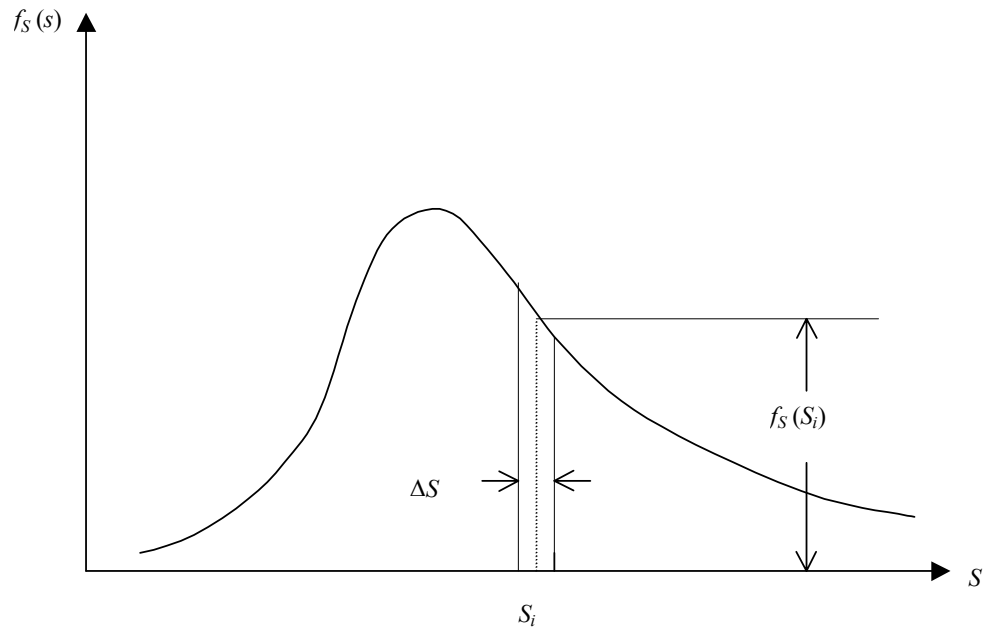
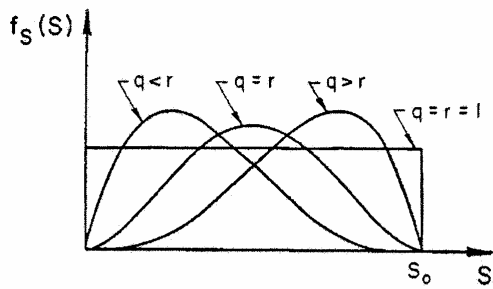
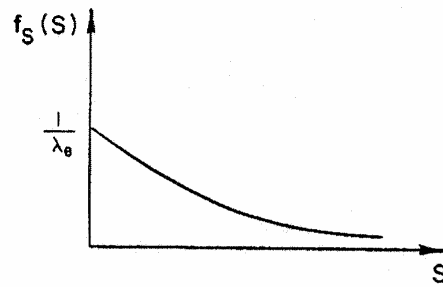


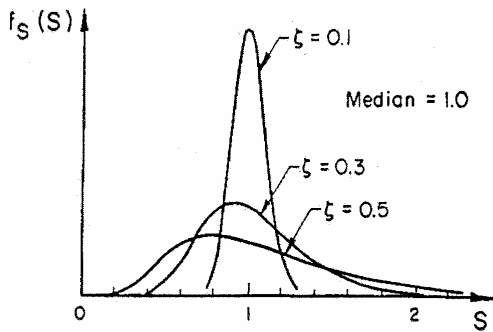
Figure 7. Probability Density Function (PDF) for Wave-induced Stress



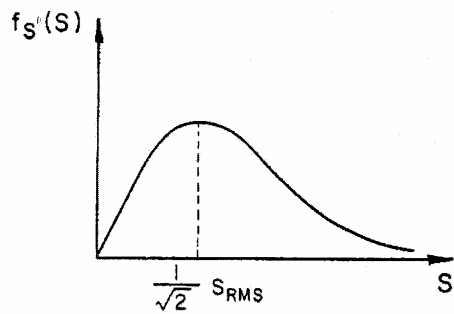
(a) Beta Distributions



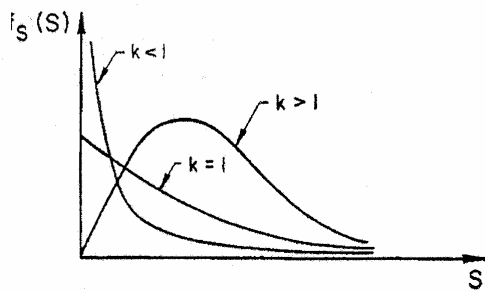
(d) Exponential Distribution



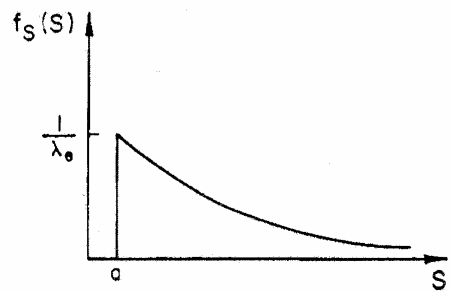
(b) Lognormal Distributions



(e) Rayleigh Distribution



(c) Weibull Distributions



(f) Shifted Exponential Distribution

Figure 8. Shapes of Probability Density Functions for Commonly Used Probability Distributions (Munse et al. 1983)

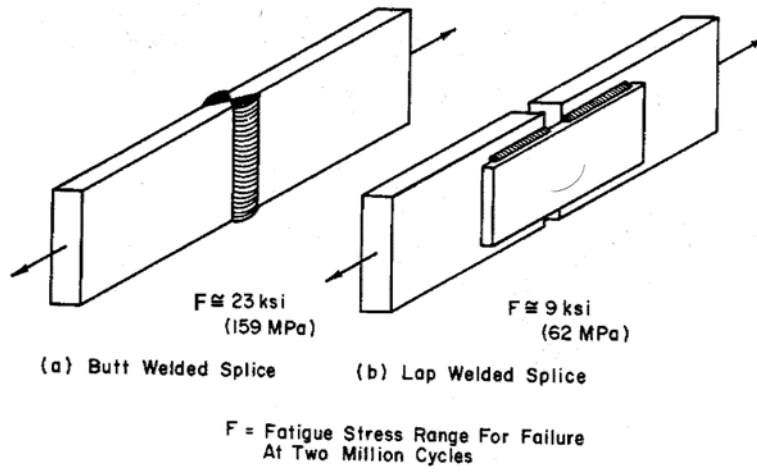


Figure 9. Welded Splice Showing Difference in Fatigue Resistance (Munse et al.1983)

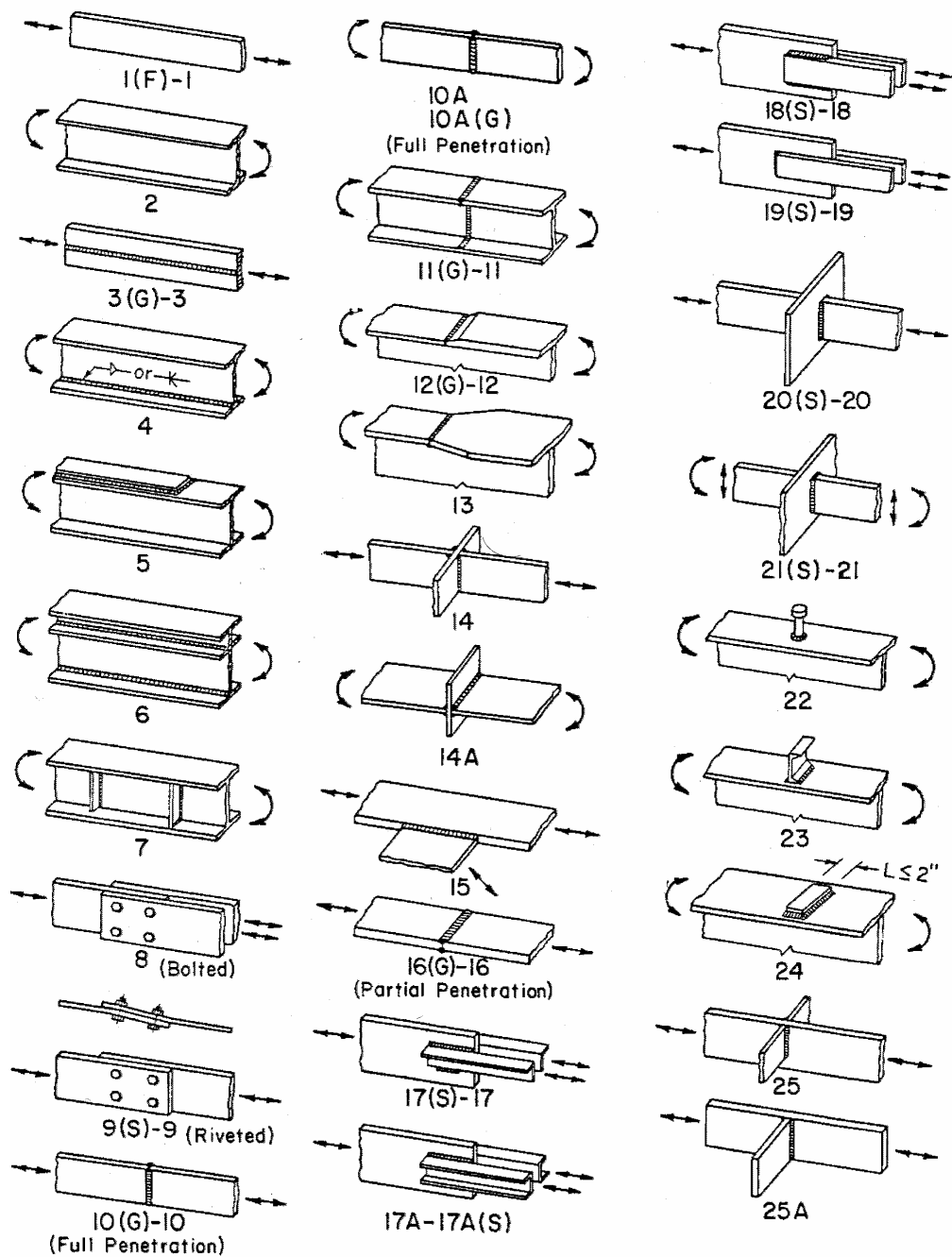


Figure 10. Structural Fatigue Details (Munse et al. 1983)

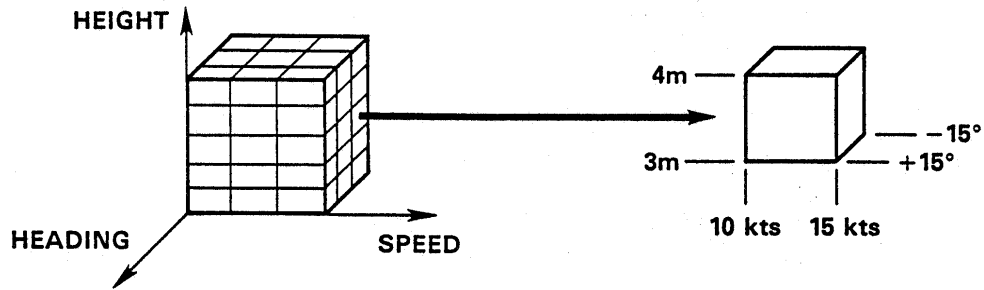


Figure 11. Operational Envelope for Ships (Sikora, et al. 1983)

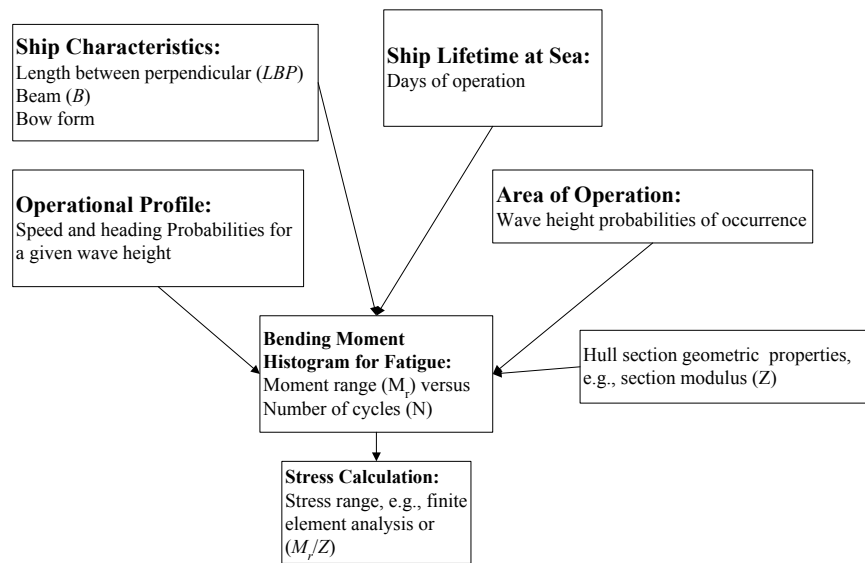


Figure 12. Response Histogram for Fatigue (Sikora et al. 1983 and Assakkaf 1998)

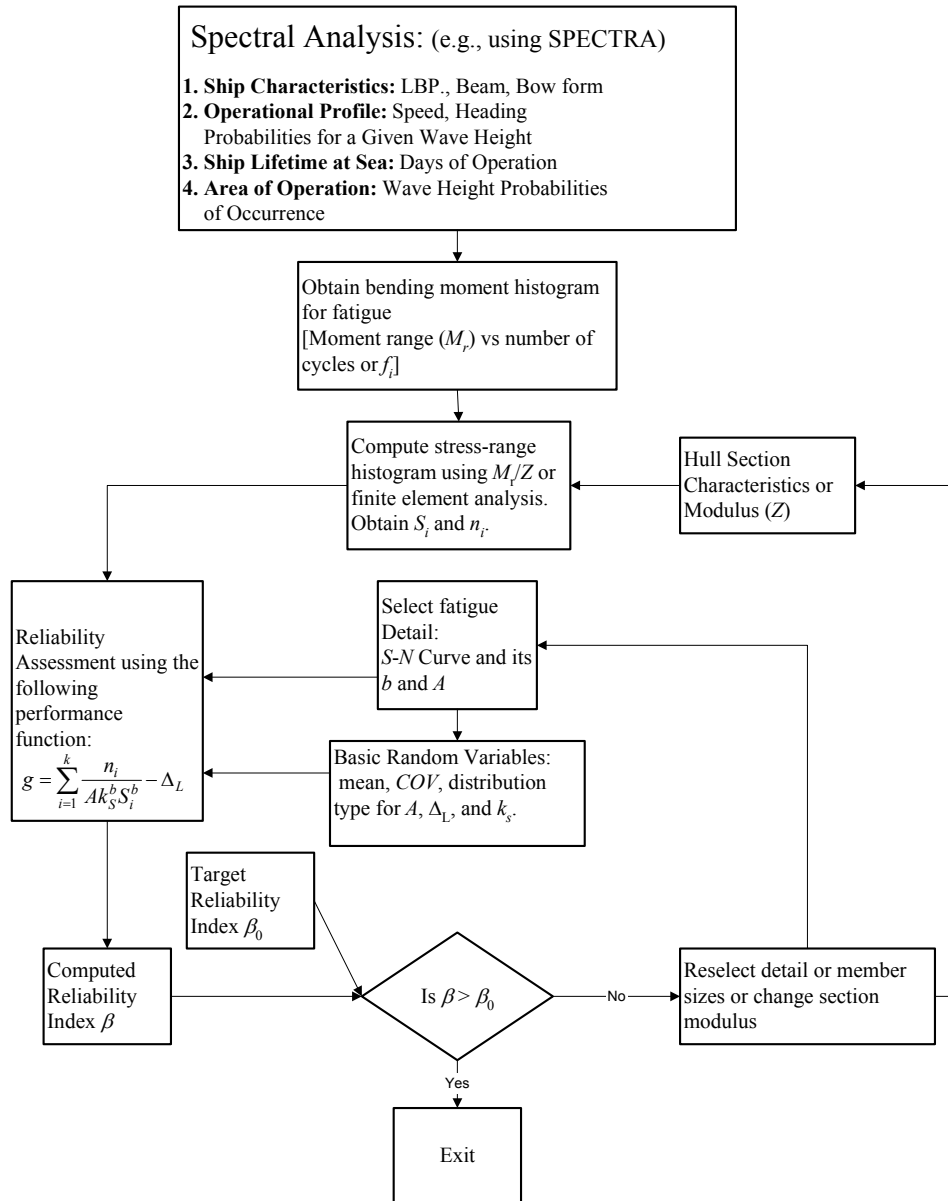


Figure 13. Direct Reliability-based Design and Analysis for Fatigue (Assakkaf 1998)

Table 1. Description of Joint Details (BS 1980 and Mansour et al. 1996)

Class	Description
B	Plain steel in the as-rolled condition, or with cleaned surfaces, but with no flame cut edges or re-entrant corners. Full penetration butt welds, parallel to the direction of applied stress, with the weld overfill dressed flush with the surface and finish-machined in the direction of stress, and with the weld proved free from significant defects by non-destructive examination
C	Butt or fillet welds, parallel to the direction of applied stress, with the welds made by an automatic submerged or open arc process and with no stop-start positions within the length. Transverse butt welds with the weld overfill dressed flush with the surface and with the weld proved free from significant defects by non-destructive examination.
D	Transverse butt welds with the welds made in the shop either manually or by an automatic process other than submerged arc, provided all runs are made in the flat position.
E	Transverse butt welds that are not class C or D.
F	Load-carrying fillet welds with the joint made with full penetration welds with any undercutting at the corners of the member dressed out by local grinding.
F2	Load-carrying fillet welds with the joint made with partial penetration or fillet welds with any undercutting at the corners of the member dressed out by local grinding.
G	Parent metal at the ends of load-carrying fillet welds which are essentially parallel to the direction of applied stress.
W	Weld metal in load-carrying joints made with fillet or partial penetration welds, with the welds either transverse or parallel to the direction of applied stress (based on nominal shear stress on the minimum weld throat area).

Table 3. Expressions of  $E(S^m)$  for Commonly Used Probability Distributions

Distribution	$E(S^m)$
Weibull	$w^m \Gamma\left(1 + \frac{m}{k}\right)$
Exponential	$\lambda_e^m \Gamma(1 + m)$
Shifted Exponential	$\sum \frac{m!}{(m-n)!} \lambda_e^n a^{m-n}$
Rayleigh	$S_{\text{RMS}}^m \Gamma\left(1 + \frac{m}{2}\right)$
Beta	$S_0^m \left[ \frac{\Gamma(m+q)\Gamma(q+r)}{\Gamma(q)\Gamma(m+q+r)} \right]$

Table 2. Properties of Commonly Used Probability Distributions (Munse et al. 1983)

Distribution Type	PDF	Characteristic Parameters	$\mu_S$	$\sigma_S$
Beta	$f_S(S) = \frac{\Gamma(q+r)}{\Gamma(q)\Gamma(r)} \frac{S^{q-1}(S_0-S)^{r-1}}{S_0^{q+r-1}}$ $0 \leq S \leq S_0$	$q, r, S_0$	$\frac{qS_0}{q+r}$	$\frac{S_0}{(q+r)} \sqrt{\frac{qr}{q+r+1}}$
Lognormal	$f_S(S) = \frac{1}{\zeta S \sqrt{2\pi}} e^{-\frac{1}{2} \left( \frac{\ln S - \lambda}{\zeta} \right)^2}$ $S \geq 0$	$\lambda, \zeta$	$e^{\lambda + \frac{1}{2}\zeta^2}$	$\sqrt{e^{\zeta^2} - 1} e^{\lambda + \frac{1}{2}\zeta^2}$
Weibull	$f_S(S) = \frac{k}{w} \left( \frac{S}{w} \right)^{k-1} e^{-\left( \frac{S}{w} \right)^k}$ $S \geq 0$	$w, k$	$w \Gamma\left(1 + \frac{1}{k}\right)$	$w \left[ \Gamma\left(1 + \frac{2}{k}\right) - \Gamma\left(1 + \frac{1}{k}\right)^2 \right]^{\frac{1}{2}}$
Exponential	$f_S(S) = \frac{1}{\lambda_e} e^{-\frac{S}{\lambda_e}}$ $S \geq 0$	$\lambda_e$	$\lambda_e$	$\lambda_e$
Rayleigh	$f_S(S) = \frac{2S}{S_{\text{RMS}}^2} e^{-\left( \frac{S}{S_{\text{RMS}}} \right)^2}$ $S \geq 0$	$S_{\text{RMS}}$	$S_{\text{RMS}} \sqrt{\frac{\pi}{2}}$	$S_{\text{RMS}} \sqrt{1 - \frac{\pi}{4}}$
Shifted Exponential	$f_S(S) = \frac{1}{\lambda_e} e^{-\frac{S-a}{\lambda_e}}$ $S \geq a$	$\lambda_e, a$	$\lambda_e + a$	$\lambda_e$

Table 4. Mean Fatigue Strength for Range of Fatigue Details of Figure 8  
(Munse et al. 1983)

Detail No.	$m$	Stress Range $S$ (ksi)			
		$N = 10^5$	$N = 10^6$	$N = 10^7$	$N = 10^8$
1(all steels)	5.729	69.40	46.50	31.10	20.80
1M	12.229	46.20	38.30	31.70	26.30
1H	15.449	56.30	48.50	41.80	36.00
1Q	5.199	80.60	51.80	33.20	21.30
1F	4.805	67.10	41.50	25.70	15.90
2	6.048	61.50	42.00	28.70	19.60
3	5.946	44.60	30.30	20.50	13.90
3(G)	6.370	44.90	31.30	21.80	15.20
4	5.663	42.50	28.30	18.80	12.50
5	3.278	26.30	13.00	6.40	3.20
6	5.663	42.50	28.30	18.80	12.50
7(B)	3.771	44.80	24.30	13.2	7.20
7(P)	4.172	35.50	20.40	11.80	6.80
8	6.549	55.80	39.20	27.60	19.40
9	9.643	32.60	25.70	20.20	15.92
L0M	7.589	34.10	25.20	18.60	13.70
10H	12.795	43.20	36.10	30.10	25.20
L0Q	5.124	48.90	31.20	19.90	12.70
10(G)	7.130	47.10	34.10	24.70	17.90
10A	5.468	47.10	31	20.30	13.30
10A(G)	--	--	--	--	--
11	5.765	33.20	22.30	14.90	10.00
12	4.398	33.20	19.60	11.60	6.9
12G	5.663	40.80	27.20	18.09	12.05
13	4.229	48.30	28.00	16.30	9.44
14	7.439	40.60	29.80	21.80	16.03
14A	--	--	--	--	--
15	4.200	24.40	14.10	8.20	4.70
16	4.631	32.80	19.90	12.10	7.37
16(G)	6.960	32.80	23.60	16.90	12.20
17	3.736	27.80	15.00	8.10	4.40
17(S)	7.782	28.20	21.00	15.60	11.60
17A	3.465	30.40	15.60	8.00	4.10
17A(S)	7.782	28.20	21.00	15.60	11.60
18	4.027	20.30	11.50	6.50	3.60
18(S)	9.233	25.70	20.00	15.60	12.20
19	7.472	23.10	17.0	12.50	9.20
19(S)	7.520	27.50	20.30	14.90	11

Table 5. Bending Moment and Stress Spectra (Sikora et al. 1983)

Bending Moment Range (k-ft)	Stress Range (ksi)	Number of Cycles
3,528,179	34.31	1
3,424,967	33.30	2
3,316,198	32.25	4
3,197,617	31.09	8
3,065,534	29.81	16
2,918,447	28.38	33
2,758,067	26.82	65
2,588,805	25.17	131
2,415,883	23.49	262
2,243,222	21.81	526
2,072,468	20.15	1,055
1,903,551	18.51	2,116
1,736,096	16.88	4,242
1,570,439	15.27	8,504
1,407,516	13.69	17,051
1,247,974	12.14	34,188
1,091,601	10.61	68,546
937,810	9.12	137,435
787,018	7.65	275,557
641,765	6.24	522,490
506,494	4.93	1,107,741
385,868	3.75	2,221,017
282,595	2.75	4,453,132
196,163	1.91	8,928,516
123,196	1.20	17,901,645

Table 6. Spectra of Wave-induced Bending Moment

Maximum Response $M_{W(sag,hag)}$	Percent max.	Cycles	log(cycles)
169,918.25	108	1	0
157,275.3	100	4.1	0.6129
141,547.77	90	21.7	1.3361
125,820.24	80	106.6	2.0278
110,092.71	70	515.3	2.7121
94,365.18	60	2,599.8	3.4149
78,637.65	50	13,650.5	4.1351
62,910.12	40	69,022.4	4.839
47,182.59	30	314,682.8	5.4979
31,455.06	20	1,270,783.5	6.1041
15,727.53	10	5,003,789	6.6993

Table 7. Spectra for Combined Wave-induced and Whipping Bending Moment

$M_{WD(hog)}$	$M_{WD(sag)}$	Cycles	log(cycles)
190,437.50	273,846.31	1	0
174,937.64	250,387.69	4.1	0.6129
155,919.72	221,816.52	21.7	1.3361
137,113.84	193,736.78	106.6	2.0278
118,357.92	165,772.80	515.3	2.7121
99,477.14	137,519.47	2,599.8	3.4149
80,479.53	108,995.37	13,650.5	4.1351
61,592.01	80,726.41	69,027.5	4.839
43,006.79	53,158.08	314,837.8	5.4981
28,309.55	34,600.57	1,272,595.4	6.1047
14,154.78	17,300.28	5,056,951.5	6.7039

Table 8. Monohull Ship Particulars (Sikora et al. 1983)

Ship	LBP (ft)	Beam (ft)	Depth (ft)	Section Modulus* (in <sup>2</sup> -ft)		Section Modulus** (in <sup>2</sup> -ft)	
				Main Deck	Keel	Main Deck	Keel
A	820	103	56.5	152,300	129,800	190,400	148,000
B	476	45.2	30.1	11,630	12,680	14,540	14,450
C	390	44.1	30.7	9,160	9,190	9,990	9,680
Mariner	520	76	48.0	17,000	23,800	17,000	23,800
SL-7	880	105.5	64.0	126,000	187,800	126,000	187,800

\* Hull Alone (From Ship Plans), \*\*Includes Deckhouse/Armor Contribution.

Table 9. Description of Joint Details (Mansour et al. 1996)

Class	Description
B	Plain steel in the as-rolled condition, or with cleaned surfaces, but with no flame cut edges or re-entrant corners. Full penetration butt welds, parallel to the direction of applied stress, with the weld overfill dressed flush with the surface and finish-machined in the direction of stress, and with the weld proved free from significant defects by non-destructive examination
C	Butt or fillet welds, parallel to the direction of applied stress, with the welds made by an automatic submerged or open arc process and with no stop-start positions within the length. Transverse butt welds with the weld overfill dressed flush with the surface and with the weld proved free from significant defects by non-destructive examination.
D	Transverse butt welds with the welds made in the shop either manually or by an automatic process other than submerged arc, provided all runs are made in the flat position.
E	Transverse butt welds that are not class C or D.
F	Load-carrying fillet welds with the joint made with full penetration welds with any undercutting at the corners of the member dressed out by local grinding.
F2	Load-carrying fillet welds with the joint made with partial penetration or fillet welds with any undercutting at the corners of the member dressed out by local grinding.
G	Parent metal at the ends of load-carrying fillet welds which are essentially parallel to the direction of applied stress.
W	Weld metal in load-carrying joints made with fillet or partial penetration welds, with the welds either transverse or parallel to the direction of applied stress (based on nominal shear stress on the minimum weld throat area).

Table 10. Statistical Data on the intercept of the  $S-N$  curve  $A$  for Joint Classification of the British Standards and the DnV

Joint Detail	$COV$ of $A$	$m$	$A$ (ksi)		Comments
			Median of $A$	Mean of $A$	
n/a	0.73	4.38	4.60 E12	--	WRC Data from RP2A (1982) commentary
n/a	1.36	4.42	1.55 E 12	--	API-X
n/a	0.50	2.88	1.04 E12	--	Butt Welded Joints
B	0.44	4.0	1.04 E12	4.47 E11	UK Den $S-N$ curves for welded joints
C	0.50	3.5	1.08 E14	4.91 E10	UK Den $S-N$ curves for welded joints
D	0.51	3.0	1.21 E10	4.64 E09	UK Den $S-N$ curves for welded joints
E	0.63	3.0	1.00 E10	3.17 E09	UK Den $S-N$ curves for welded joints
F	0.54	3.0	5.28 E09	1.92 E09	UK Den $S-N$ curves for welded joints
F2	0.56	3.0	3.75 E09	1.31 E09	UK Den $S-N$ curves for welded joints
G	0.43	3.0	1.73 E09	7.63 E08	UK Den $S-N$ curves for welded joints
W	0.44	3.0	1.12 E09	2.88 E08	UK Den $S-N$ curves for welded joints

Table 11. Statistical Information on Fatigue Damage Ratio at Failure  $\Delta$  (Wirsching and Chen 1988, and White 1992)

Median of $\Delta$	$COV$ of $\Delta$	Comments
0.90	0.67	Survey of variable amplitude fatigue data
1.00	0.60	Survey of random tests:
0.70	0.60	Large quasi-static mean load change
1.15	0.48	Full-scale cover-plated steel beams
0.85	0.28	Longitudinal non-load carrying fillet welds
0.78	0.19	Non-load carrying welds
1.06	0.40	Non-load carrying fillet welds
0.69	0.61	Cruciform specimen

Table 12. Ranges for the mean and  $COV$  of the fatigue Damage Ratio at Failure  $\Delta$

	Median of $\Delta$	$COV$ of $\Delta$
Minimum	0.69	0.19
Recommended	0.90	0.48
Maximum	1.15	0.67

Table 13. Partial Safety Factors for Category B of the British Standards (BS 5400)

$\beta_0$	$\phi_A$	$\phi_A$	$\gamma_{ks}$	$\gamma_S$
2.0	0.55	0.60	1.09	1.10
2.5	0.48	0.53	1.11	1.12
3.0	0.42	0.48	1.13	1.15
3.5	0.37	0.43	1.15	1.18
4.0	0.32	0.38	1.17	1.21

Table 14. Partial Safety Factors for Category W of the British Standards (BS 5400)

$\beta_0$	$\phi_A$	$\phi_A$	$\gamma_{ks}$	$\gamma_S$
2.0	0.52	0.57	1.07	1.08
2.5	0.45	0.50	1.09	1.10
3.0	0.39	0.45	1.11	1.12
3.5	0.34	0.40	1.13	1.15
4.0	0.29	0.35	1.14	1.17

Table 15. Probabilistic Characteristics of Random Variables for Detail No. 5 of Munse et al. (1983)

Random Variable	Mean	COV	Distribution Type
$S_e$	6.96 ksi	0.10	Lognormal
$\Delta$	1.0	0.48	Lognormal
$A$	4.47 E09	0.40	Lognormal
$k_s$	1.0	0.10	Normal
$m$	3.278	na	na
$\beta$	2.5	na	na

na = not applicable

Table 16. Probabilistic Characteristics of Random Variables for Detail No. 7(P) of Munse et al. (1983)

Random Variable	Mean	COV	Distribution Type
$S_e$	7.95 ksi	0.10	Lognormal
$\Delta$	1.0	0.48	Lognormal
$A$	2.88 E11	0.40	Lognormal
$k_s$	1.0	0.10	Normal
$m$	4.172	na	na
$\beta$	2.5	na	na

na = not applicable

Table 17. Probabilistic Characteristics of Random Variables for Detail # 27(S) of Munse et al. (1983)

Random Variable	Mean	COV	Distribution Type
$S_e$	9.13 ksi	0.10	Lognormal
$\Delta$	1.0	0.48	Lognormal
$A$	1.15 E12	0.40	Lognormal
$k_s$	1.0	0.10	Normal
$M$	5.277	na	na
$\beta$	2.5	na	na

na = not applicable

Table 18. Probabilistic Characteristics of Random Variables for Class B Detail (BS)

Random Variable	Mean	COV	Distribution Type
$S_e$	27.54 ksi	0.10	Lognormal
$\Delta$	1.0	0.48	Lognormal
$A$	4.47 E11	0.44	Lognormal
$k_s$	1.0	0.10	Normal
$M$	4.0	na	na
$\beta$	2.5	na	na

na = not applicable

Table 19. Results of Reliability Checking for Fatigue Design (Target  $\beta = 2.5$ )

Detail No.	$m$	Mean $A$ ( $\bar{A}$ )	$\bar{S}_e$	Computed $\beta$	Reliability Checking
5	3.28	4.47 E09	6.96	5.6	acceptable
7(P)	4.17	2.88 E11	7.95	7.5	acceptable
27(S)	5.28	1.15 E12	9.13	4.8	acceptable
Class B	4.0	4.47 E11	27.5	2.3	unacceptable

na = not applicable

Table 20. Results Using Direct Reliability-Based Fatigue Design (Target  $\beta = 2.5$ )

Selected Detail	Computed Mean Value of $S_e$ ( $\bar{S}_e$ )
5	14.10
7(P)	20.71
27(S)	13.57
Class B	26.27

<b>RELIABILITY-BASED DESIGN GUIDELINES FOR FATIGUE OF SHIP STRUCTURES .....</b>	<b>1</b>
<b>ABSTRACT.....</b>	<b>1</b>
<b>1. INTRODUCTION.....</b>	<b>2</b>
<b>2. LIMIT STATES AND DESIGN STRENGTH.....</b>	<b>4</b>
2.1 THE FRACTURE MECHANICS APPROACH.....	5
2.2 THE CHARACTERISTIC <i>S-N</i> APPROACH .....	6
2.3 NOMINAL STRESS VERSUS HOT SPOT STRESS .....	7
2.4 MINER’S RULE AND THE EQUIVALENT STRESS RANGE CONCEPT .....	8
2.5 PERFORMANCE FUNCTIONS FOR FATIGUE .....	10
2.5.1 <i>Life Cycle Formulation</i> .....	12
2.5.2 <i>Fatigue Damage Ratio Formulation</i> .....	12
2.6 FATIGUE DETAILS .....	14
<b>3. DESIGN LOADS .....</b>	<b>16</b>
3.1 SPECTRAL ANALYSIS .....	16
3.2 BENDING MOMENT AND STRESS SPECTRA.....	18
<b>4. RELIABILITY-BASED DESIGN GUIDELINES FOR FATIGUE .....</b>	<b>19</b>
4.1 TARGET RELIABILITY LEVELS .....	19
4.2 STATISTICAL CHARACTERISTICS OF FATIGUE RANDOM VARIABLES.....	19
4.2.1 <i>Uncertainty in Fatigue Strength</i> .....	19
4.2.2 <i>Fatigue Details and Data</i> .....	21
4.2.2.1 British Standards and DnV Structural Details	21
4.2.2.2 Statistical Data on Fatigue Details as Given by Munse et al. (1983)	21
4.2.2.3 Statistical Information on Fatigue Damage Ratio D	22
4.3 SAMPLE LRFD GUIDELINES .....	22
4.3.1 <i>Direct Reliability-Based Design</i> .....	22
4.3.1.1 Direct Reliability-Based Design Method	22
4.3.1.2 Reliability Checking for Fatigue	23
4.3.1.3 Computation of Reliability-based Design Stress	24
4.3.2 <i>Load and Resistance Factor Design</i> .....	24
<b>5. DESIGN EXAMPLE .....</b>	<b>26</b>
<b>6. SUMMARY AND CONCLUSIONS .....</b>	<b>26</b>
<b>ACKNOWLEDGMENTS.....</b>	<b>27</b>
<b>REFERENCES.....</b>	<b>27</b>